CONF-940713--3

SAN095-1354C

DISCLAIMER

SOL-GEL STRATEGIES FOR AMORPHOUS INORGANIC MEMBRANES EXHIBITING MOLECULAR SIEVING CHARACTERISTICS

N. K. Raman [1], C. J. Brinker[1,2], L. Delattre[1], and S.S. Prakash[1]
[1]UNM/NSF Center for Micro-Engineered Ceramics
Farris Engineering Center, The University of New Mexico
Albuquerque, NM 87131
[2]Sandia National Laboratories, Advanced Materials Laboratory
1001 University Blvd. SE, Albuquerque, NM 87106

Abstract

We have used several sol-gel strategies to prepare supported inorganic membranes by a process that combines the features of slip-casting and dip-coating. To be practically viable the deposited membranes must exhibit both high flux and high selectivity. For porous membranes these requirements are met by extremely thin, defect-free porous films exhibiting a narrow size distribution of very small pores.

This paper considers the use of polymeric silica and hybrid-organosilyl precursor sols in the context of the underlying physics and chemistry of the membrane deposition process. Since the average membrane pore size is ultimately established by the collapse of the gel network upon drying, it is necessary to promote polymer interpenetration and collapse during membrane deposition in order to achieve the very small pore sizes necessary for molecular sieving. For polymeric sols, this is accomplished using rather weakly branched polymers characterized by fractal dimension $D < 1.5$ under deposition conditions in which the silica condensation rate is minimized. By analogy to organic polymer sols and gels, we believe that the breadth of the pore size distribution can be influenced by the occurrence of micro-phase separation during membrane deposition. Minimization of the condensation rate not only fosters polymer collapse but should inhibit phase separation, leading to a narrower pore size distribution.

The formation of microporosity through collapse of the gel network requires that small pores are achieved at the expense of membrane porosity. Incorporation of organic template ligands within a dense silica matrix followed by their removal allows us to independently control pore size and pore volume through the size and volume fraction of the organic template. Such strategies can be used to create microporous films with large volume fraction porosities.

Introduction

Both zeolites and silica glasses are inorganic frameworks composed of rings of $M(O_{0.5})_4$ tetrahedra. In zeolites, the rings are aligned in one, two, or three dimensions, creating uniform channels that can support adsorption and diffusion. The size of the ring, to a first approximation, governs the channel diameter or aperture size. For example, regular rings of four to twelve tetrahedra in zeolite structures create apertures ranging from 0.16 to 0.8 nm in diameter, respectively. The combination of small aperture size with the inherent rigidity of the inorganic framework causes the transport of asymmetric molecules to exhibit both entropic and diffusional barriers, leading to potentially large separation factors. D_{O2}/D_{N2} is reported to exceed 100 for Type A zeolite in which the main aperture is formed by an eight-membered ring with aperture 0.43 nm [1]. Thus, zeolites would appear to be excellent candidate materials for molecular sieving membranes.

Unfortunately, it is difficult to process zeolites into ultra-thin defect free layers necessary to achieve high flux and high selectivity. Conventional hydrothermal syntheses of zeolites performed on porous alumina supports require crystallite intergrowth to eliminate intragranular porosity. This results in layers often tens of micrometers thick. In addition it is difficult to imagine using hydrothermal processing to fabricate inorganic membranes that could compete economically with conventional organic membranes. For these reasons, we have focused our attention on preparing ultramicroporous, amorphous silica membranes using sol-gel processing techniques.

As in zeolites, amorphous silicates are composed of rings of connected tetrahedra. The most common ring size in *fully dense* amorphous silica is six, corresponding to an aperture of 0.28 nm, but unlike zeolites there is a distribution of ring sizes and the rings are not aligned into channels. Qualitatively, sol-gel silica prepared by an acid-catalyzed procedure and processed below about 700°C can be considered a *dilated* amorphous silica with somewhat larger average ring size. Transport through sol-gel silica is expected to be dominated by the pathway of largest connected rings. If every such pathway has constrictions created by eight-membered rings, we might anticipate separation characteristics similar to Type A zeolite. The advantage of sol-gel processing over zeolite synthesis is that preparation of ultrathin, defect-free layer is comparatively simple.

This paper first describes some of the physicochemical phenomena that influence film thickness, defect formation, and pore size in sol-gel derived films or membranes. We then describe an organic template approach to prepare silica membranes that can potentially lead to membranes combining high flux and high selectivity.

Sol-Gel Membrane Formation

Properties of Sol-Gel Derived Silica Membranes

The location, thickness, porosity, and pore size of the deposited membranes prepared by dip-coating depends on a variety of factors including: 1) the size and structure of the inorganic species contained in the sol; 2) the pore size of the support;

3) withdrawal rate U; 4) sol concentration, viscosity, and surface tension; 5) relative rates of condensation and evaporation; and 6) the balance between the capillary pressure, which compacts the gel structure, and the gel modulus or viscosity, which resists compaction, during the final stage of drying [2]. The influence of these factors on the structure of the deposited membrane is discussed in the following subsections.

Location: The ultimate location of the inorganic components of the sol deposited by slip-casting and substrate withdrawal depends on the relative sizes of the particles or polymers in the sol and the pore size of the support. Fig. 1 shows a series of cross-sectional TEM images of silica membranes deposited on 4-nm Membralox® γ-Al_2O_3 supports [3]. Aging was used to vary the size of the silica polymers prior to dip-coating. When the Guinier radius R_G of the polymers determined by small angle x-ray scattering (SAXS) is significantly smaller than the pore radius of the support, we observe no evidence of a membrane layer on the support surface. In this situation, silica deposition occurs exclusively within the support. However, when R_G is comparable to or exceeds the support pore size, a discrete membrane layer is formed on the support surface. As the average polymer size increases, silica is more efficiently collected on the support surface, leading to thicker external layers. Correspondingly, EDS analyses indicate less silica deposition within the underlying support [3].

Thickness: The mass of the membrane deposited per unit area depends on contributions from both slip-casting and substrate withdrawal. The corresponding membrane thickness depends on the membrane location and porosity. Slip-casting occurs by flow of liquid into the underlying support. The entrained condensed phase deposits on (or within) the support. Assuming that slip-casting occurs exclusively through flow of liquid into the ~4-μm thick γ-Al_2O_3 support layer to form a discrete silica deposit of density 2.0 g/cm^3, we calculate the slip-cast layer thickness to be equal to 35 nm for a sol of concentration 0.6 M SiO_2 equivalent.

Withdrawal of the support entrains a sol layer on the support surface. The layer thickness h represents a three-way balance between viscous force, gravity, and surface tension as expressed in the following relationship [4]:

$$h = 0.94(\eta U)^{2/3}/\gamma_{LV}^{1/6}(\rho g)^{1/2} \qquad (1)$$

where ρ is the sol density and g is the acceleration of gravity. For a withdrawal rate U = 0.67 cm/s and typical viscosity, surface tension, and density for an alcohol/water-based sol of equivalent silica concentration 0.6 M (η= 2 centipoise, γ_{LV}= 22.7 dyn/cm, and ρ = 0.79 g/cm^3), h = 7.1 μm. This entrained layer thins by gravitational draining and evaporation. Assuming that the entrained sol is concentrated to a discrete silica film of density 2.0 g/cm^3 during drying, the membrane thickness attributable to substrate withdrawal is 126 nm. Based on the above discussion, we see that, by judicious choice of sol polymer size and deposition conditions, it is relatively simple to prepare discrete, ultra-thin (<< 1 μm) membrane layers.

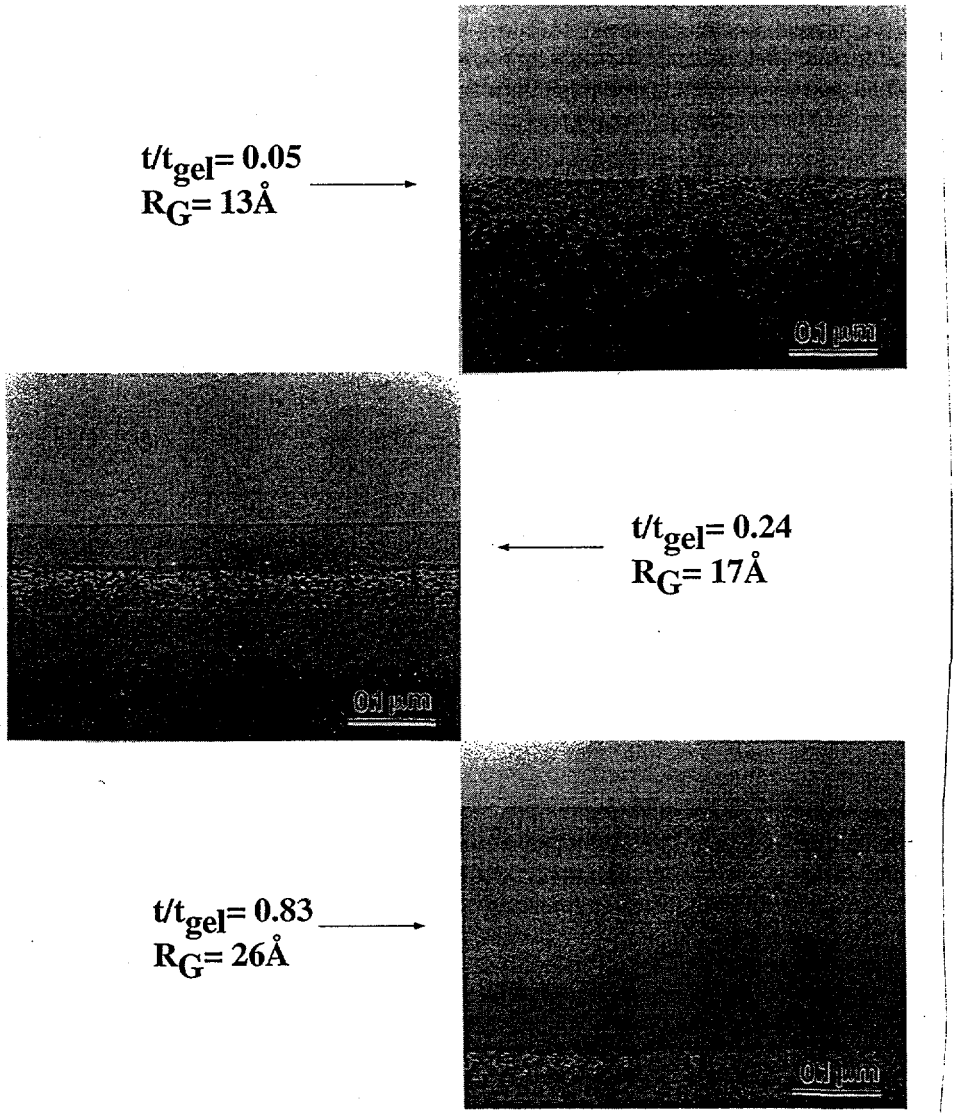

Figure 1: Cross-sectional TEM micrographs of silica membranes deposited on 4-nm γ-Al_2O_3 tubular supports as a function of sol aging time.

The essential microstructural features of the deposited membrane, viz. pore volume, pore size, and pore size distribution depend on the structure of the gel and its response to the capillary pressure. Considering only polymeric sols, *small, uniform pores necessary to achieve molecular sieving are obtained under conditions*

that favor uniform polymer packing and promote collapse during drying. For polymeric sols characterized on the mesoscopic length scale by a mass fractal dimension D, the packing efficiency of the polymers confined within the thinning liquid film should depend inversely on their points of contact. For two fractal objects of size R and fractal dimension $D1$ and $D2$ placed in the same region of space, the mean number of intersections $M_{1,2}$ is expressed as [5]:

$$M_{1,2} \propto R^{D1 + D2 - d} \tag{2}$$

where d is the dimension of space. From Eq. 2 we see that if $D1 + D2 < 3$, the probability of intersection decreases indefinitely with R. This suggests that, as D is reduced, polymers should more easily interpenetrate as they are concentrated during membrane deposition, leading to the formation of a uniform "intertwined" network.

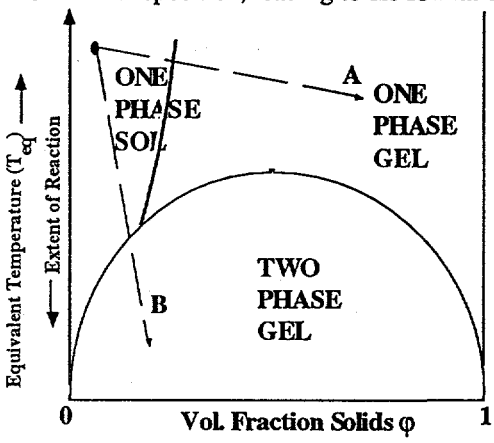

Figure 2: Equivalent phase diagram of a polymer gel in semi-dilute solution with a good solvent [6].

Condensation reactions that accompany drying influence the evolving microstructure of the membrane in several ways: 1) condensation reactions that occur at points of intersection impede polymer interpenetration; 2) condensation reactions increase the sol viscosity prior to gelation, promote chemical gelation, and increase the elastic moduli after gelation. Each of these factors serves to resist compaction of the gel network by the capillary pressure; 3) based on consideration of the equivalent phase diagram for a polymer gel in semi-dilute solution with good solvent (Fig. 2) [6], condensation reactions accompanying solvent evaporation may cause the trajectory of the reaction path to cross the coexistence line (Path B in Fig. 2) rather than traverse the single phase sol to gel phase boundary (Path A). Although crosslinking of the gel prevents a macroscopic phase separation, the gel probably experiences at this point a "microphase separation" that serves to broaden the pore size distribution for equivalent pore volumes and average pore sizes [3].

Establishment of Pore Size: The most important microstructural feature of microporous membranes is the average pore size. For bulk gels, it is believed that the final pore size is established at the critical point where drying shrinkage stops due to the balance of the maximum capillary tension in the liquid $P_C = -\gamma_{LV}\cos(\theta)/r_p$ and the compressive stress on the network [7].

At the critical point where shrinkage stops, the volumetric strain ε_V of the gel network attributable to drying is [7]:

$$\varepsilon_V = \frac{\sigma_Y}{K_p} = \left(\frac{1 - \phi_S}{K_p}\right)\left(\frac{-\gamma_{LV}\cos(\theta)}{r_p}\right) \quad (3)$$

where K_p is the bulk modulus of the network. For a wide variety of silica gels it has been shown that the modulus depends on the strain as a power law [7]:

$$K_p = K_0(V_0/V)^m, \quad (4)$$

where V_0 and V are the initial and shrunken volumes of the gel, K_0 is the initial bulk modulus of the gel, and m = 3.0-3.8.

For membrane deposition the situation is similar except that substantial drying can precede gelation causing the pore sizes to be appreciably smaller than observed in bulk gels. In this case the maximum capillary tension depends on the relative pressure of the pore fluid according to the Kelvin equation.

Based on the above discussion, a simple strategy emerges for the preparation of microporous membranes from polymeric silica sols: 1) the catalyst concentration is chosen to minimize the condensation rate, 2) the hydrolysis and aging conditions are chosen so the polymer size exceeds the support pore size, while maintaining $D <$ ~1.5, and 3) deposition conditions are chosen to maximize P_C. Under these conditions, polymers can be grown large enough to be trapped on the support surface. As the sol is concentrated by evaporation, the polymers should freely interpenetrate, leading to a uniform physical gel structure with little tendency to phase separate. The gel should remain compliant throughout most of the drying period, allowing it to be compacted by the capillary pressure to a relatively dense state $\phi_S \geq 0.9$ characterized by a small average pore radius $r_p \leq 1.0$ nm and narrow pore size distribution.

This basic strategy has been successfully demonstrated by Uhlhorn et. al. [8] and de Lange et. al. [9] for silica membrane deposition on polished γ-Al_2O_3 disk supports. In this proceedings, Sehgal et. al. [10] have demonstrated that this strategy provides amorphous silica membranes that mimic molecular sieving behavior of zeolites.

Organic Template Approaches

A limitation of the polymeric approach described above is that small pores necessary for molecular sieving are achieved by promoting collapse of the gel network and therefore elimination of porosity. Thus higher separation factors are achieved at the expense of flux. This situation can be remedied using the "organic template" approach whereby non-hydrolyzable organic ligands are introduced in the inorganic framework to promote collapse of the gel to a dense state followed by ligand removal to create a microporous membrane.

In this way it should be possible to achieve rather large volume fractions of pores of the appropriate size for molecular sieving, overcoming the limitation identified above. The major challenges of this approach are to obtain a dense matrix prior to template removal and to achieve pore connectivity, for example by exceeding the percolation threshold of the templates, while avoiding phase

separation that upon template removal would create pores larger than individual template ligands.

Experimental - Organic ligands were introduced into polymeric silica sols by co-condensation of tetraethoxysilane (TEOS) 1 with methyltriethoxysilane (MTES) 2 or methacryloxypropylsilane (MPS) 3 (Fig. 3) using two-step acid-catalyzed procedures. For the TEOS/MTES system, the first step consisted of mixing TEOS + MTES, ethanol, water, and 1M HCl in the molar ratio 1:3.8:1.1:0.0007 and refluxing

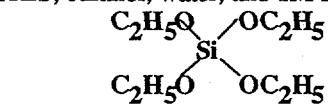

1 Tetraethylorthosilicate (TEOS)

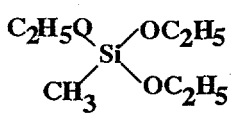

2 Methyltriethoxysilane (MTES)

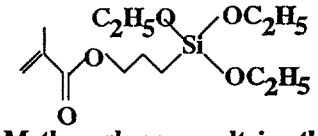

3 Methacryloxypropyltrimethoxysilane (MPS)

Figure 3: Structure of the precursors used in the organic template approach.

at 60°C for 90 min with stirring. In the second step additional water and 1M HCl were added at room temperature resulting in the final ratio of 1:3.8:5.1:0.056. For the TEOS/MPS system, the first step consisted of mixing TEOS, MPS, ethanol, water, and HCl in the molar ratio 0.8:0.2:1.1:3.8:4.9 x 10^{-5} and refluxing at 60°C for 90 min. with stirring. In the second step water and HCl were added, resulting in the final molar ratio 0.8:0.2:5.1:4.2 x 10^{-3}. After aging the sols at 50°C for times corresponding to t/t_{gel} = 0.05 to 0.85, the sols were diluted 2:1 with ethanol (vol. EtOH:vol sol).

For the TEOS/MTES system, membranes were prepared on Membralox® support tubes as described previously [11] and calcined in air at temperatures between 150 and 550°C for 0.5 or 4 h with heating and cooling rates of 1°C/min. After performing permeability measurements, the membranes were impregnated with a dilute solution of TEOS monomer and re-calcined. Single-gas permeabilities of the supports and membranes were measured at room temperature as a function of pressure using helium, carbon dioxide, nitrogen, methane, and sulfur hexafluoride with kinetic diameters of 2.65, 3.3, 3.64, 3.8, and 5.5Å, respectively.

For the TEOS/MPS system, the sol was poured on a plastic petridish to form a film 1.5 mm in thickness. After drying at room temperature the film was crushed and calcined in air to 150°C or 500°C using a heating rate of 1°C/min. Nitrogen adsorption isotherms were acquired using a Micromeritics ASAP 2000 micropore analyzer.

Results and Discussion:

After drying at 150°C for 0.5 h, the as-deposited membranes exhibited separation factors greater than ideal Knudsen values for He/N_2, He/SF_6, and

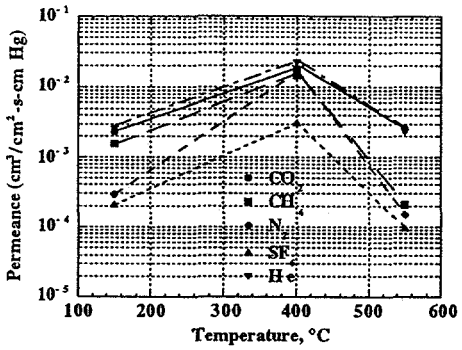

Figure 4: Permeance data of 10 mol% MTES/TEOS membranes as a function of calcination temperature. The line is a visual guide.

CO_2/CH_4. The permeances increased with temperature suggestive of molecular sieving. As shown in Fig. 4, the permeances of all the gases increased and the separation factors decreased somewhat after calcination at 400° C to remove the ethoxy ligands. However after calcination at 550°C to remove the methyl ligands the permeances of all the gases decreased dramatically compared to CO_2 and He. These results indicate that densification of the matrix combined with the removal of template ligands creates microporous channels within a dense inorganic matrix [12]. The pores created are of molecular dimensions as evidenced by separation factors exceeding ideal Knudsen values. The transport behavior of the TEOS/MTES membranes was modified by impregnation with 1:12 TEOS monomer (vol. TEOS : vol. EtOH) solution. After impregnation and calcination in air at 400°C for 4 hours the separation factors of gas pairs He/SF_6, He/N_2, and CO_2/CH_4 (as summarized in Table 1) greatly exceeded ideal Knudsen values. We infer from these results that the impregnation step healed the defects and/or narrowed the pore size distribution in the underlying membrane layer causing a significant enhancement in the separation factors with only a modest reduction in the permeance values.

Table 1 Ideal Separation factors and He permeances (cm^3/cm^2-s-cm Hg) of the 10 mol% MTES/TEOS membranes as a function of calcination temperature

	Calcination Temperature	He Permeance	He/N_2	He/SF_6	CO_2/CH_4
Knudsen Selectivity			2.65	6.0	0.6
After first coating	150°C	$2.55x10^{-3}$	8.7	12.1	1.5
	400°C	$2.24x10^{-2}$	1.3	7.2	1.2
	550°C	$2.31x10^{-3}$	15.4	24.3	12.2
After Impregnation	400°C	$1.32x10^{-4}$	14.4	328	71.5

As shown in Fig. 5a, the nitrogen adsorption isotherm acquired for the TEOS/MPS film after heating to 150°C was of Type II indicative of no accessible porosity on the experimental time scale. After heating to 500°C, where TGA data show pyrolysis of the organic constituents to be complete, the adsorption isotherm is

distinctly of Type I indicating the formation of a microporous material. The low relative pressure adsorption data (inset Fig. 5b) is consistent with an extremely narrow pore size distribution.

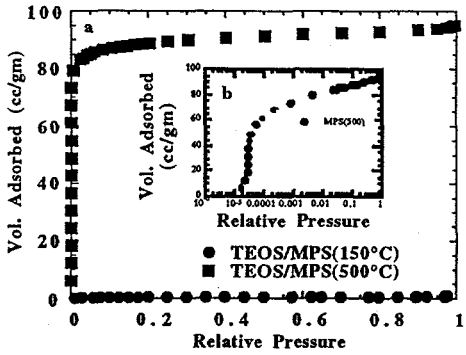

Figure 5: N_2 adsorption isotherms at 77K for TEOS/MPS (4:1) as a function of heat treatment. Inset (5b) shows the isotherm at the low relative pressure (10^{-6} - 1) for the 500°C heat treated sample.

These results demonstrate the feasibility of the organic template approach to create microporous silica. The major distinction between these two systems is the hydrophobicity/ hydrophilicity of the template ligand and its possible influence on phase separation and the magnitude of P_c during membrane deposition. For both systems, we expect that the composition of the pore fluid will be enriched in water during drying [13]. Consequently, in the case of TEOS/MTES, the hydrophobic methyl ligand (2) could induce incipient phase separation and increase the contact angle θ, reducing P_c. These combined phenomena could inhibit compaction of the matrix and "lump together" the template ligands, consistent with experimental findings. By comparison, we expect the hydrophilic methacryloxypropyl ligands (3) to have the reverse effect, leading to dense structures with uniform incorporation of organic ligands. Compared to films and membranes prepared from tetraalkoxysilanes (1), it appears that the non-hydrolyzable organic ligand promotes compaction of the structure during drying, probably by reducing K_O, K_p or m (see Eqs. 3 and 4).

Summary

In supported silica membranes prepared from polymeric precursors, the size of the polymer with respect to the pore size of the support governs the location of the membrane layer. The membrane pore size and pore size distribution are influenced by factors that determine how densely and uniformly the polymers pack together during the deposition process. In general reduction of the mass fractal dimension and condensation rate and increase of the capillary pressure lead to denser structures with smaller pore sizes and narrower pore size distributions. The final pore size of the membrane is established by a balance of the rising capillary stress due to drying and the increasing network modulus or viscosity due to shrinkage. Through the use of organic templates, it appears feasible to prepare membranes that combine high porosity and small pore size necessary to achieve high flux and high selectivity in membrane applications. However in this case, we anticipate that the membrane structure may be additionally strongly influenced by organic ligand/solvent interactions.

Acknowledgments

The authors acknowledge financial assistance from NSF (CTS9101658), the Electric Power Research Institute, the Gas Research Institute, and Morgantown Energy Technology Center. Sandia National Laboratories is a U.S. DOE facility supported by contract No. DE-AC04-76-DP00789.

References

1. D. W. Breck, Zeolite Molecular Sieves, Krieger Pub. Co., Malabar, FL, 1984.

2. C.J. Brinker and G.W. Scherer, Sol-gel Science: The physics and chemistry of sol-gel processing, Academic Press, San Diego, 1990.

3. C. J. Brinker, R. Sehgal, N. K. Raman, P. R. Schunk, and T. J. Headley, *J. Sol-Gel Sci. & Tech.*, 2, 469-476, (1994).

4. L. D. Landau and B. G. Levich, *Acta Physiochim*. URSS 17, (1942) 42-54.

5. B.B. Mandelbrot, The Fractal Geometry of Nature, W. H. Freeman and Company, New York, 1982.

6. P.G. deGennes, Scaling Concepts in Polymer Physics, Cornell University Press, New York, 1991.

7. G. W. Scherer, *J. Non-Cryst. Solids,* 155, (1993) 1-25.

8. R.J.R. Uhlhorn, K. Keizer, and A.J. Burggraaf, "Gas transport and separation with ceramic membranes," *J. Membrane Sci.*, 76 [2 & 3], (1992), 271-288.

9. R.S.A. de Lange, "Microporous sol-gel derived ceramic membranes for gas separation: synthesis, gas transport and separation properties," *Ph.D. Thesis*, University of Twente, Enchede, The Netherlands 1993.

10. R. Sehgal, J. C. Huling, C. J. Brinker, this proceedings.

11. C.J. Brinker, T.L. Ward, R. Sehgal, N.K. Raman, S.L. Hietala, D.M. Smith, D.-W. Hua, and T.J. Headley, *J. Membrane Sci.*, 77, (1993) , 165-179.

12. N. K. Raman and C. J. Brinker, "Organic "template" approach to molecular sieving silica membranes," *J. Membrane Sci.*, in press.

13. F. Nishida, J. M. McKiernan, B. Dunn, J. I. Zink ,C. J. Brinker, and A. J. Hurd, *J. Sol-Gel Sci. & Tech.*, in press.